

Article

Self-Assembly of High Density of Triangular Silver Nanoplate Films Promoted by 3-Aminopropyltrimethoxysilane

Norhayati Abu Bakar ^{1,*}, Joe George Shapter ^{2,*}, Muhamad Mat Salleh ¹ and Akrajas Ali Umar ¹

¹ Institute of Microengineering and Nanoelectronics (IMEN),
Universiti Kebangsaan Malaysia, 43600 Bangi, Selangor, Malaysia;
E-Mails: mms@ukm.edu.my (M.M.S.); akrajas@ukm.edu.my (A.A.U.)

² School of Chemical and Physical Sciences and Flinders Centre for Nanoscale Science and
Technology, Flinders University, Bedford Park, Adelaide South Australia 5001, Australia

* Authors to whom correspondence should be addressed; E-Mails: nab_yati@yahoo.com (N.A.B.);
joe.shapter@flinders.edu.au (J.G.S.); Tel.: +60-3-8911-8548 (N.A.B.); +61-8-8201-2005 (J.G.S.);
Fax: +60-3-8925-0439 (N.A.B.); +61-8-8201-2905 (J.G.S.).

Academic Editor: Philippe Lambin

Received: 29 May 2015 / Accepted: 16 July 2015 / Published: 30 July 2015

Abstract: In this work, we studied the structure of synthesized triangular silver nanoplates in solution and the growth of the nanoplates on a silicon surface using 3-aminopropyltrimethoxysilane (APTMS) as a coupling agent. The triangular-shaped colloidal silver nanoplates were simply synthesized by a direct chemical reduction approach. We studied the three characteristic peaks of the unique optical absorbance of triangular silver nanoplates and subsequently measured an average edge length of 26 ± 1 nm. The nanoplate thickness was determined to be 7 ± 2 nm from transmission electron microscopy images. Depositing the nanoplates on a silicon surface was carried out to determine the coverage of triangular nanoplates obtained when adhesion was promoted by a coupling agent. The APTMS film assisted the attachment of the nanoplates to the silicon surface and the coverage of the nanoplates increased with increasing deposition time. The triangular silver nanoplate thin film was a monolayer and a high coverage (near complete) was obtained after eight hours of exposure to the nanoplate solution. The silver film formed was shown to be a good surface-enhanced Raman scattering (SERS) substrate as it gave an enormous Raman enhancement for bisphenol A (BPA).

Keywords: 3-aminopropyltrimethoxysilane (APTMS); high density surface; self assembly; triangular silver nanoplate thin film

1. Introduction

Research in synthetic control of noble metal nanoparticles has proven to be a powerful and versatile approach for tailoring the properties of the metal nanostructures for various applications [1–3]. Silver nanoparticles have been prepared with various techniques to modify their optical, electrical, and catalytic properties, which are strongly dependent on the shape and size of the silver nanoparticles. Much effort from many research groups has examined the synthesis of silver colloidal solutions with suspensions of various shapes and sizes including silver nanospheres [4,5], nanowires [6,7], nanoplates [8,9], nanocubes [10], and nanorods [11]. Among these nanostructures, silver nanoplates have attracted considerable attention because they could potentially generate maximum electromagnetic field enhancement due to their highly anisotropic structure [12–14]. As a result, these particles are ideal for implementation in sensing applications including localized surface plasmon resonance (LSPR) [15–18], surface-enhanced fluorescence [19], and surface-enhanced Raman scattering (SERS) [20–22], which are possibly the most attractive applications.

In contrast, solution-based synthesis of anisotropic nanostructures has not been suitably applied for device applications including sensing analysis. Generally, the sensing analysis has been done by directly mixing the silver colloids with the analyte solution [23]. Therefore, silver is considered to be a single use system as opposed to multiple uses for a silver thin film [24]. The silver thin film can easily be washed to remove the analyte from the surface to allow a second or potentially repeated analysis and this result alternatively helps to prove the repeatability of the sensing system. Additionally, understanding the growth of the silver thin films is crucial in the fabrication of devices including solar cells and light emitting diodes (LEDs) because the growth on solid surfaces is influenced by the specific size, shape, and distribution of the nanostructures being deposited [25,26].

The growth of anisotropic nanostructures on solid surfaces has been reported using various methods such as thermal growth, seed-mediated growth, self-assembly, and lithography [27]. Recently, interest in surface modification in thin film fabrication has increased because control of the degree of coverage and aggregation of the nanostructures is possible and will allow the construction of a SERS substrate. A variety of organic materials can self-assemble on solid surfaces to obtain a molecular layer on the surface which promote the attachment of nanostructures to surfaces [28,29]. 3-Aminopropyltrimethoxysilane (APTMS) is a common aminosilane used to promote metal nanostructure adhesion on the surface due to the strong interactions between the amine group and the metal nanoparticles [30,31].

Hence, the aim of this work is to deposit silver nanoplates on a silicon surface with maximum surface coverage of the triangular nanoplates using self-assembly with an adhesion layer. The distribution of the triangular silver nanoplates was studied by varying the exposure time of the silver nanoplate solution to the silicon surface. The silver nanoplate thin film was attached to the silicon surface using an APTMS film as a coupling agent in order to enhance the adhesion between the surface and the nanoplates. The morphology of the samples was investigated using field emission scanning electron microscopy (FESEM).

2. Experimental Section

2.1. Chemicals

The chemicals used to prepare the triangular silver nanoplate suspension include silver nitrate (Sigma Aldrich, Kuala Lumpur, Malaysia), trisodium citrate (Wako Pure Chemical Industries, Ltd.: Osaka, Japan), 30% hydrogen peroxide (HmbG Chemicals), and sodium borohydride (Sigma Aldrich). Meanwhile, 3-aminopropyltrimethoxysilane 97% (Sigma Aldrich) and ethanol absolute (HmbG Chemicals, Kuala Lumpur, Malaysia) were used to functionalize the silicon surface. These chemicals were utilized as received without any further purification.

2.2. Synthesis and Fabrication of Monolayer Triangular Silver Nanoplate Thin Film

The triangular silver nanoplate solution was prepared via a direct chemical reduction approach at ambient temperature in air. A typical synthesis process is described in the following: 0.2 mL of 0.05 M silver nitrate (AgNO_3) was mixed into 96.56 mL of deionized water. Then, the solution was vigorously stirred by a magnetic stirrer at 900 rpm. After that, 2.0 mL of 75 mM trisodium citrate was mixed into the solution followed by 0.24 mL of 30% hydrogen peroxide (H_2O_2). To start a reduction process of Ag ions to Ag metal, 0.1 M sodium borohydride (NaBH_4) was injected quickly into the stirred solution. The ultimate stable formation of triangular silver nanoplates in solution can be roughly seen through the color change of the solution. A clear, colorless solution changed to a dark blue solution after vigorously stirring for 5 min. This solution was then subjected to ultrasonic treatment for 1 h at 27 °C. The output power of ultrasonic bath is about 160 Watts. Afterward, the solution was centrifuged at 6000 rpm for 30 min. A pellet eventually formed at the bottom of centrifuge tube and the pellet was extracted to make the solutions used in the deposition of triangular nanoplate films on the silicon surface.

The monolayer triangular silver nanoplate film was grown on the silicon surface by a self-assembly technique. This approach was typically started by cleaning a silicon substrate via immersing in piranha solution for 1 h to remove any organic waste on the silicon surface. Next, the substrate was cleaned in acetone and then in ethanol with ultrasonic treatment for 15 min. After that, the clean silicon was immersed in 5% 3-aminopropyltrimethoxysilane (APTMS) in ethanol for 1 h at room temperature to functionalize the silicon surface. The APTMS film on silicon substrate was then rinsed with copious amounts of ethanol and the surface was dried. Finally, this APTMS film was heated on a hot plate for 2 h at 100 °C. The deposition of the triangular nanoplates on the silicon surface was done by immersing the APTMS-covered silicon into a silver nanoplate solution formed by redissolving the centrifuged pellet in water.

To study changes in surface coverage of the triangular nanoplates on the surface, the exposure time of the APTMS-covered silicon to the nanoplate suspensions was varied from 15 min to 22 h. The films were then characterized using atomic force microscopy, AFM (Veeco, Riverside, CA, USA), and field emission scanning electron microscopy, FESEM (Hitachi, Kuala Lumpur, Malaysia), to determine the morphology and coverage of the monolayer triangular silver nanoplate thin films. Meanwhile, transmission electron microscopy, TEM (Philips, New South Wales, Australia), optical absorbance (Cary 5G spectrophotometer; Varian, Melbourne, Australia), and dynamic light scattering, DLS (HPLS Maples, Adelaide, Australia), were recorded for the silver nanoplate solution to study the shape and

size of the triangular nanoplates. The SERS measurement was recorded using a Raman spectrometer (Horiba Scientific, New South Wales, Australia) with a 532 nm excitation laser wavelength with 10 seconds integration time.

3. Results and Discussion

Triangular silver nanoplates were successfully prepared by direct chemical reduction at room temperature as reported by Zhang [32]. The formation of the nanoplates was simply obtained by the reduction of silver ion to silver from silver nitrate by a reduction agent, namely sodium borohydride. This shape formation was effectively controlled by trisodium citrate and hydrogen peroxide. The triangular nanoplate formation could be roughly observed via color change when sodium borohydride was injected into the colorless solution which contained silver nitrate, trisodium citrate, and hydrogen peroxide. The solution color changed to yellowish after 1 min during the reduction process. The color continued to change for five minutes until the color remained dark blue. The centrifuged silver nanoplate pellet was resuspended and then was characterized to study the optical properties, uniformity of shape, and particle size.

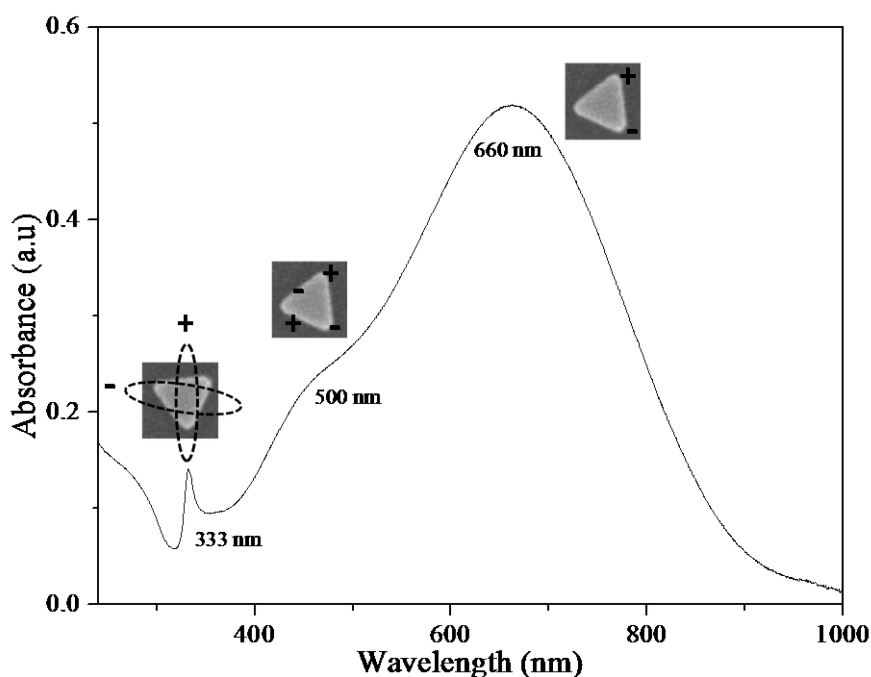


Figure 1. Optical absorbance with corresponding mode of plasmon excitation of resuspended triangular silver nanoplate solution.

The optical properties of the silver nanoplates were studied using the surface plasmon resonance of the particles, which can be probed using the absorbance spectrum. This resonance has a strong dependence on the shape of particles [33]. The resuspended silver nanoplate suspension was characterized by UV-Vis and the optical absorbance spectrum is shown in Figure 1. Based on the absorbance spectrum, it was found that the triangular silver nanoplates exhibited a sharp plasmon band at 333 nm and an intense broad surface plasmon situated at 660 nm along with a shoulder at around 500 nm.

In Figure 1, the corresponding modes of plasmon excitation for each extinction peak of the solution are also provided. The three characteristic peaks correspond to different modes of plasmon excitation of triangular nanoplates [34]. The two dominant bands located at 333 nm and 660 nm are due to the out-of-plane quadrupole resonance and in-plane dipole resonance, respectively. The shoulder at 500 nm is a result of the formation of anisotropic nanoparticles and it is attributed to the in-plane quadrupole resonance of silver nanoplates. These three modes of plasmon excitation agree with the structure of the triangular nanoplate shown in the observed TEM images (Figure 2a).

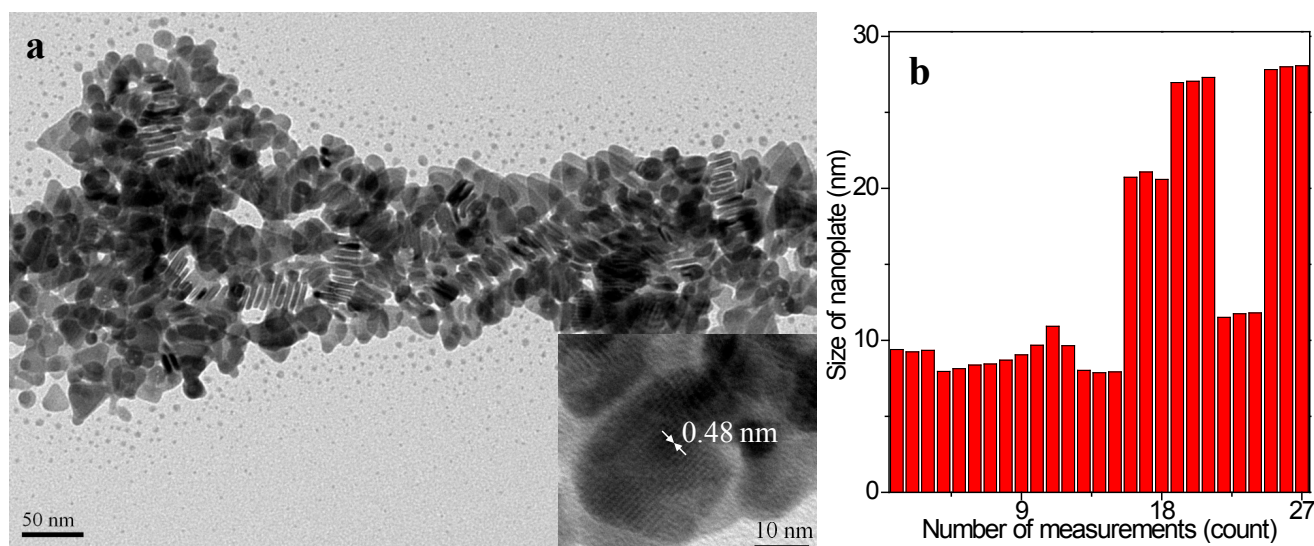


Figure 2. Triangular silver nanoplate solution (a) TEM image; the inset picture shows the lattice spacing of triangular nanoplates and (b) size distribution from dynamic light scattering (DLS) measurements.

The resuspended triangular silver nanoplate solution was dropped on a cuprum grid surface for TEM characterization. The solution was first dried at room temperature for 10 min prior to imaging. Figure 2a shows an image of triangular nanoplates that was captured with 120 kV. However, it is difficult to observe the triangular shape because the nanoplates have a tendency to stack face-to-face via self-assembly during the evaporation of the solvent in preparing the TEM sample. The uniform thickness of the plates can be seen from this stacking formation and this allowed determination of the plate size. This size measurement was analyzed using iTEM software (Adelaide, Australia), and the average plate thickness is 7 ± 2 nm while the average edge length of triangular nanoplates is 26 ± 1 nm. The inset figure in Figure 2a shows the captured lattice of nanoplates when imaged by TEM. The perfect lattice was measured at 0.48 nm, which corresponds to the lattice spacing of face-centered cubic (FCC) silver crystal. The growth direction of nanoplates corresponding to this measured lattice spacing is likely to be the $\langle 111 \rangle$ direction based on the X-ray diffraction (XRD) Bruker XRD D8 Advance; (Selangor, Malaysia) characterization [35]. Given this is the most stable FCC crystal plane, this is the growth direction that would be expected.

The average size of triangular nanoplates was also confirmed using dynamic light scattering (DLS) as plotted in Figure 2b. This bar chart for the size of the nanoplate particles vs. the number of measurements for each size was determined from DLS measurements by determining the frequency of

occurrence of each particle size (based on volume) over 27 scans of the same colloidal silver nanoplate suspension. It was found that the size of the nanoplates varied. This is due to the fact that DLS measured two length parameters: thickness and edge length of the triangular nanoplate structure. The average edge length of nanoplates was determined by DLS to be 25 ± 3 nm, while the average plate thickness was found to be 9 ± 1 nm. These measurements agreed closely with TEM results.

Triangular silver nanoplate thin films on a silicon surface were grown via a self-assembly technique. Prior to exposing the nanoplate solution to the surface, the clean silicon surface was functionalized by immersing the surface in 5% 3-aminopropyltrimethoxysilane (APTMS) solution for 1 h. The APTMS film formed on surface was used to promote adhesion between the substrate and the silver nanoplates. APTMS has been used as a good coupling agent for the modification of silica surfaces to attach silver triangular nanoplates due to the robust interaction between the amine group and metal nanoparticles as reported by Howarter [36]. As a result, a silver nanoplate film was successfully deposited on the silicon surface after 15 min of exposure time, as shown in the FESEM image in Figure 3a.

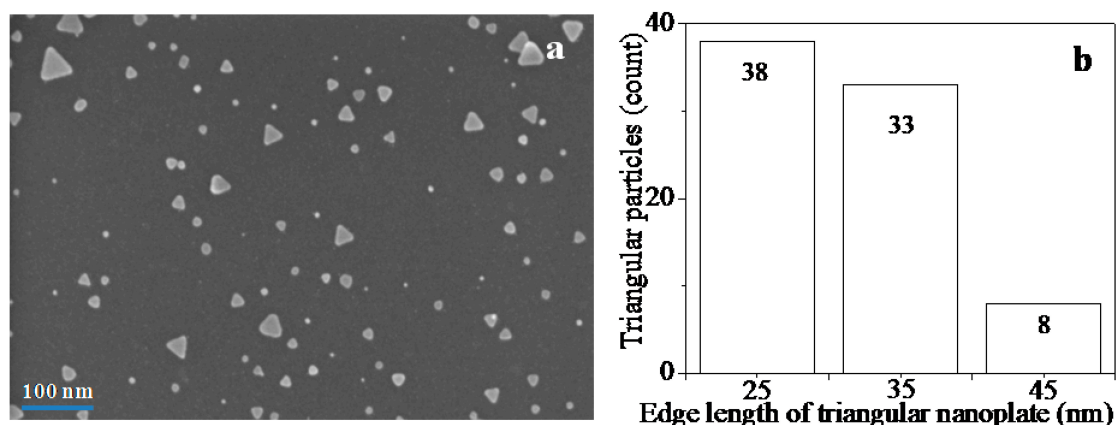


Figure 3. (a) FESEM image of nanoplate film on silicon surface after 15 min of exposure; (b) Bar chart for edge length of triangular nanoplates for 15 min growth on surface. The edge length of 25 means the size of nanoplates was from 20 to 30 nm, 35 from 30 to 40 nm, and 45 from 40 to 50 nm.

The FESEM image clearly proves that the film of silver nanoplates was starting to grow on the surface after just 15 min of exposure to the nanoplate solution, with a high yield of triangular shapes due to the presence of the silane molecule. It should be noted that both AFM and FESEM imaging of the untreated and treated silicon substrates were featureless (please refer to supplementary material). Additionally, similar imaging showed that exposure of the nanoplate solution to an untreated substrate lead to no deposition. Hence, the silane molecule on the surface did assist the attachment of the silver nanoplates because there is no distribution of nanoplates on the surface without the APTMS layer. The silver nanoparticles were electrostatically attached to aminosilane molecules due to the silver in the solution interacting with the APTMS-covered silicon surface [37,38]. The image also reveals that the triangular nanoplates are well attached to the silicon surface and the nanoplates are not agglomerated. The average edge length of triangular nanoplates is 25.05 ± 7.37 nm, which was calculated using image J software. The different edge lengths of triangular nanoplates determined through SEM images

are plotted in Figure 3b. The results found that the edge length of 25 nm was the most common size observed on the surface and agreed with TEM and DLS analysis.

The growth of the nanoplate film on the surface was studied for different exposure times. Freshly silanized surfaces were immersed for 30 min, 1 h, 2 h, 8 h, 14 h, and 22 h in the nanoplate solution. Figure 4 shows the FESEM images of the nanoplate thin film on the surface after various exposure times. It was found that the density of nanoplates on the surface increased with increasing exposure time. From these coverage examples, it is clear that the attachment of APTMS on the surface ultimately enhanced the growth of nanoplates on the surface. The triangular nanoplate film grew with high affinity for the all exposure times. Thus, nanoplate films were successfully formed on the surface with the nanoplates unlikely to overlap with each other and thus be well organized in a monolayer on the silicon surface.

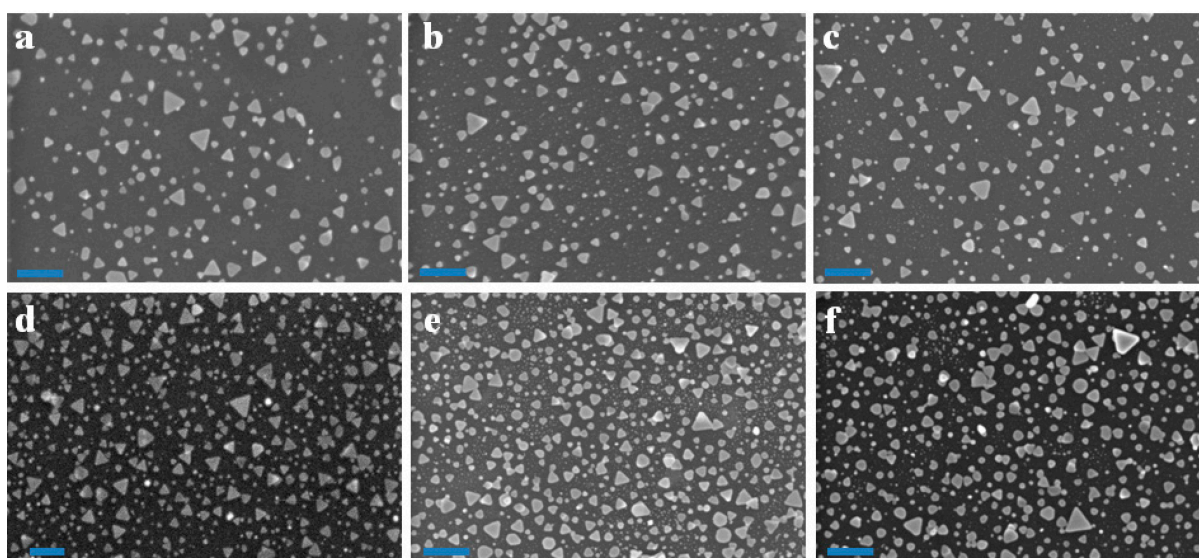


Figure 4. FESEM images of triangular silver nanoplate thin films formed after varying exposure times of (a) 30 min, (b) 1 h, (c) 2 h, (d) 8 h, (e) 14 h, and (f) 22 h. Scale bar is 100 nm.

Silver nanoparticles with spherical and irregular shapes did start to appear on the surface after 8 h of immersion in the nanoplate solution. The irregular shapes were readily observed in 14 h and 22 h exposure time samples. It should be noted that for these samples, the distribution of triangular nanoplate shapes on the surface is still higher than the distribution of irregular shapes on surface. The formation of irregular shapes with increasing exposure times is likely related to the increasing coverage of nanoplates on the surface. This increased density means that it is possible that the nanoplates begin to coalesce when the neighboring particles get close to each other [39]. From the measurement of triangular nanoplate sizes, we calculated that the ratio of irregular to triangular shapes is 20:80 for both samples.

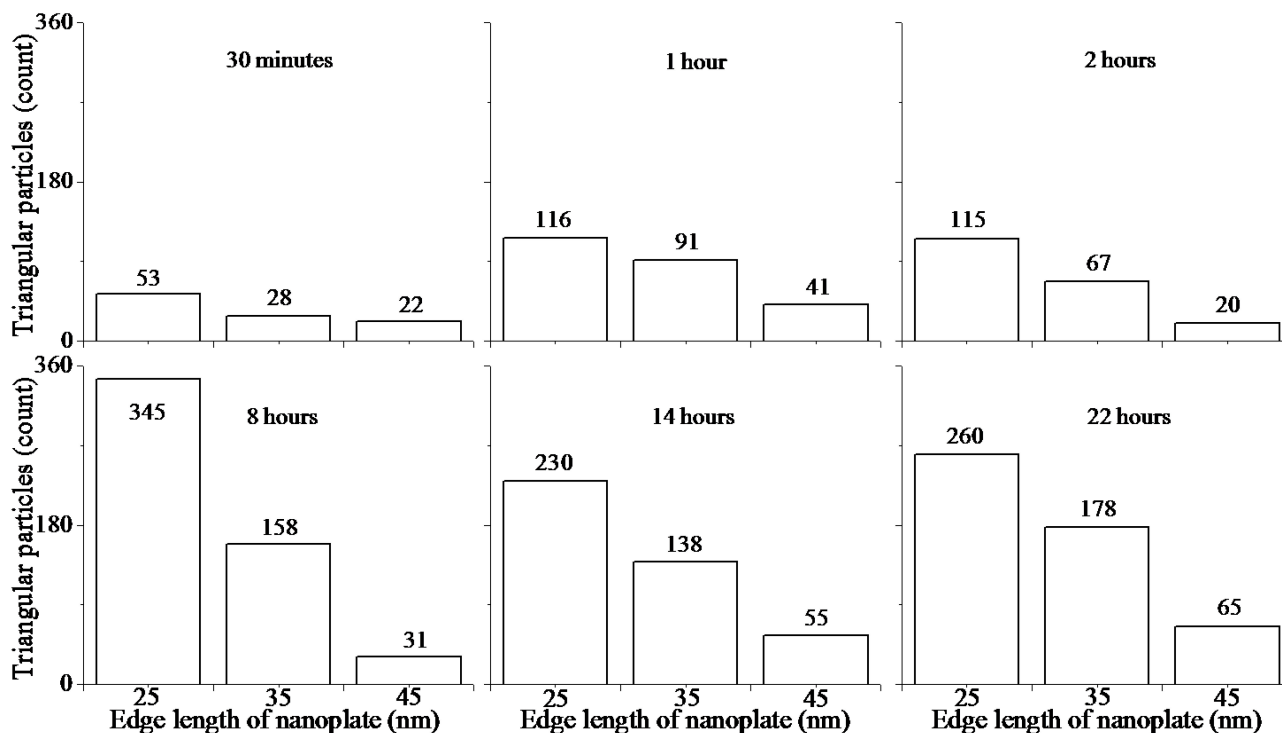


Figure 5. The edge length of triangular nanoplates on the surface for different exposure times. The edge length of 25 means the size of the nanoplates was from 20 to 30 nm, 35 from 30 to 40 nm, and 45 from 40 to 50 nm.

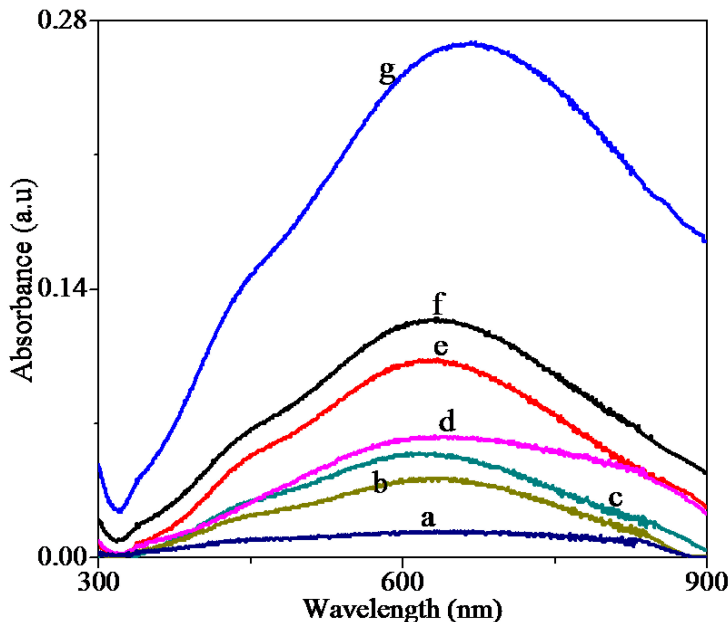


Figure 6. Optical absorbance for silver nanoplate films formed after the various exposure times of (a) 15 min, (b) 30 min, (c) 1 h, (d) 2 h, (e) 8 h, (f) 14 h, and (g) 22 h.

The size of the particles on the surface was analyzed using the same approach as the 15 min sample and the analysis results are plotted in Figure 5 and given in Table 1. Importantly, the average edge length of triangular nanoplates for different exposure times did not change. However, the count of

triangular nanoplates increased with exposure time, showing the density of nanoplates on surface increases with exposure time.

The optical properties of the silver nanoplate films formed after different exposure times were studied by observing their absorbance spectra, which are presented in Figure 6. In the suspension there were three clear peaks at 330 nm, 550 nm, and 660 nm (see Figure 1). The signal from the substrate-bound nanoplate films is much weaker, as expected, as the optical characterization was done on the thin silver nanoplate films instead of the concentrated nanoplates in the suspension. However, for the sample with the highest coverage (produced after 22 h of substrate exposure), a broad surface plasmon at 660 nm was observed along with two shoulders at 330 nm and 550 nm. These peaks align closely with the spectrum of the suspension, further confirming the presence of the nanoplates on the substrate. Additionally, the intensity of the absorbance increased with increasing exposure time due to the increasing coverage of the nanoplates, as revealed by the SEM images.

Table 1. The measurement of the edge length and the coverage of triangular nanoplates on the surface for 15 min to 22 h samples of exposure times.

Exposure Times	Edge Length of Nanoplates (nm)	Coverage of Nanoplates on the Surfaces (Counts/ μm^2)
15 min	25.05 \pm 7.37	79
30 min	25.59 \pm 9.72	103
1 h	26.21 \pm 8.40	248
2 h	24.37 \pm 7.37	202
8 h	27.47 \pm 6.68	534
14 h	25.24 \pm 7.49	423
22 h	25.11 \pm 7.68	503

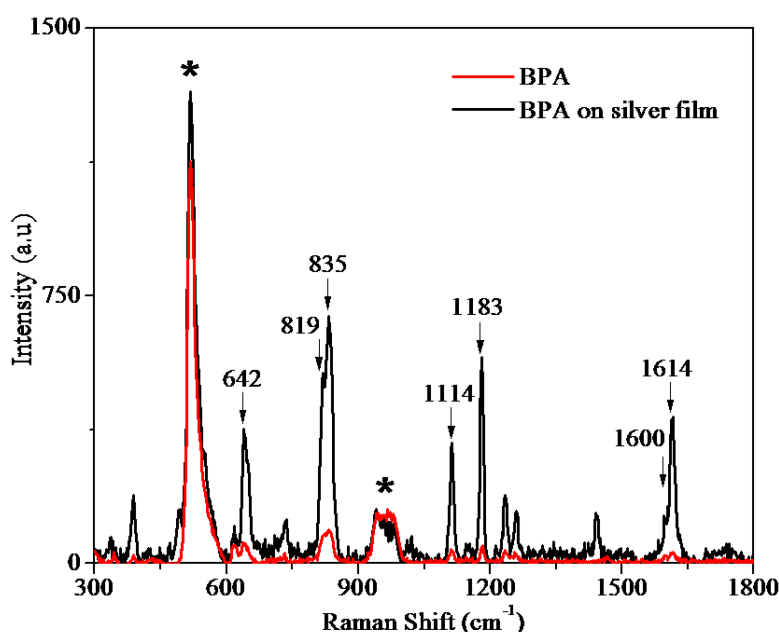


Figure 7. The SERS spectrum of BPA on the silver nanoplate film (formed after 2 h exposure time) and Raman of BPA absorbed on a clean silicon surface. * are labels for the silicon peaks.

Figure 7 shows the SERS spectrum of 1 mM bisphenol A (BPA) on the silver nanoplate film formed after exposing the substrate to the nanoplate suspension for 2 h. The normal Raman spectrum for 1 mM BPA on the silicon surface is also provided in Figure 7. As expected, BPA shows seven major Raman peaks at 642 cm^{-1} , 819 cm^{-1} , 835 cm^{-1} , 1114 cm^{-1} , 1183 cm^{-1} , 1600 cm^{-1} , and 1614 cm^{-1} , clearly indicating the presence of BPA on the substrate [40]. These BPA peaks were strongly enhanced when the molecule was absorbed on the silver nanoplate film, clearly demonstrating that these nanoplate films are a good SERS substrate and suitable for further investigations for incorporation in a SERS-based sensor.

4. Conclusions

Silver nanoplates with a triangular shape were successfully synthesized using direct chemical reduction. The optical properties exhibited a unique optical absorbance with two major bands and one shoulder, which are attributed to dipole resonance and quadrupole resonance due to the triangular nanoplate's shape. The assembly of the nanoplates on a silicon surface with an APTMS layer was studied for seven different exposure times. We found that for longer exposure times, the coverage of the triangular nanoplates on the surface increased, but the average size of the individual plates remained constant. For longer exposure times, some irregular-shaped particles were observed on the surface. However, the eight-hour exposure did produce a triangular silver nanoplate thin film with a high density surface. These thin films are promising for applications in SERS detectors as demonstrated by the enhanced signal obtained for bisphenol A absorbed on the silver nanoplate film.

Acknowledgments

We thank the Malaysian Ministry of Higher Education and Universiti Kebangsaan Malaysia for financial grants of ERGS/1/2012/STG02/UKM/01/1. Norhayati Abu Bakar would like to thank Flinders University for funding to support travel and lab access. This work is supported by the Australian Microscopy and Microanalysis Research Facility (AMMRF).

Author Contributions

Norhayati Abu Bakar performed the experiment and wrote the paper. Joe George Shapter participated in data analysis and ideas, revised the manuscript, and provided the facilities. Muhamad Mat Salleh and Akrajas Ali Umar provided the facilities and discussed the results.

Conflicts of Interest

The authors declare no conflict of interest.

References

1. Zeng, J.; Zheng, Y.; Rycenga, M.; Tao, J.; Li, Z.Y.; Zhang, Q.; Zhu, Y.; Xia, Y. Controlling the shapes of silver nanocrystals with different capping agents. *J. Am. Chem. Soc.* **2010**, *132*, 8552–8553.

2. Jin, M.; He, G.; Zhang, H.; Zeng, J.; Xie, Z.; Xia, Y. Shape-controlled synthesis of copper nanocrystals in an aqueous solution with glucose as a reducing agent and hexadecylamine as a capping agent. *Angew. Chem. Int. Edit.* **2011**, *50*, 10560–10564.
3. Tsuji, M.; Gomi, S.; Maeda, Y.; Matsunaga, M.; Hikino, S.; Uto, K.; Tsuji, T.; Kawazumi, H. Rapid transformation from spherical nanoparticles, nanorods, cubes, or bipyramids to triangular prisms of silver with PVP, Citrate, and H₂O₂. *Langmuir* **2012**, *28*, 8845–8861.
4. Taleb, A.; Petit, C.; Pileni, M.P. Synthesis of highly monodisperse silver nanoparticles from AOT reverse micelles: A way to 2D and 3D self-organization. *Chem. Mater.* **1997**, *9*, 950–959.
5. Krutyakov, Y.A.; Kudrinskiy, A.A.; Olenin, A.Y.; Lisichkin, G.V. Synthesis and properties of silver nanoparticles: Advances and prospects. *Russ. Chem. Rev.* **2008**, *77*, 233–257.
6. Sun, Y.; Gates, B.; Mayers, B.; Xia, Y. Crystalline silver nanowires by soft solution processing. *Nano Lett.* **2002**, *2*, 165–168.
7. Caswell, K.K.; Bender, C.M.; Murphy, C.J. Seedless, surfactantless wet chemical synthesis of silver nanowires. *Nano Lett.* **2003**, *3*, 667–669.
8. Ledwith, D.M.; Aine, M.W.; John, M.K. A Rapid, straight-forward method for controlling the morphology of stable silver nanoparticles. *J. Mater. Chem.* **2007**, *17*, 2459–2464.
9. Lim, G.H.; Han, I.; Yu, T.; Lim, B. Aqueous-phase synthesis of silver nanoplate: Enhancing lateral growth via a heat-up process. *Chem. Phys. Lett.* **2013**, *568*, 135–139.
10. Zhang, Q.; Huang, C.Z.; Ling, J.; Li, Y.F. Silver nanocubes formed on ATP-mediated nafion film and a visual method for formaldehyde. *J. Chem. Phys. B* **2008**, *112*, 16990–16994.
11. Guo, S.; Dong, S.; Wang, E. Rectangular silver nanorods: Controlled preparation, liquid-liquid interface assembly, and application in surface-enhanced Raman scattering. *Cryst. Growth Des.* **2009**, *9*, 372–377.
12. Kelly, K.L.; Coronado, E.; Zhao, L.L.; Schatz, G.C. The optical properties of metal nanoparticles: The influence of size, shape, and dielectric environment. *J. Chem. Phys. B* **2003**, *107*, 668–667.
13. Zhang, X.Y.; Hu, A.; Zhang, T.; Lei, W.; Xue, X.J.; Zhou, Y.; Duley, W.W. Self-assembly of large-scale and ultrathin silver nanoplate films with tunable plasmon resonance properties. *ACS Nano* **2011**, *5*, 9082–9092.
14. Li, N.; Zhang, Q.; Quinlivan, S.; Goebel, J.; Gan, Y.; Yin, Y. H₂O₂-aided seed-mediated synthesis of silver nanoplates with improved yield and efficiency. *ChemPhysChem* **2012**, *13*, 2526–2530.
15. Pastoriza-Santos, I.; Liz-Marzán, L.M. Colloidal silver nanoplates. State of the art and future challenges. *J. Mater. Chem.* **2008**, *18*, 1724–1737.
16. Si, G.; Shi, W.; Li, K.; Ma, Z. Synthesis of PSS-capped triangular silver nanoplates with tunable SPR. *Colloids Surf. A* **2011**, *380*, 257–260.
17. Zhang, J.; Sun, Y.; Zhang, H.; Xu, B.; Zhang, H.; Song, D. Preparation and application of triangular silver nanoplates/chitosan composite in surface plasmon resonance biosensing. *Anal. Chim. Acta* **2013**, *769*, 114–120.
18. Brandon, M.P.; Ledwith, D.M.; Kelly, J.M. Preparation of saline-stable, silica-coated triangular silver nanoplates of use for optical sensing. *J. Colloid Interf. Sci.* **2014**, *415*, 77–84.
19. Folmar, M.; Shtoyko, T.; Fudala, R.; Akopova, I.; Gryczynski, Z.; Raut, S.; Gryczynski, I. Metal enhanced fluorescence of Me-ADOTA Cl dye by silver triangular nanoprisms on a gold film. *Chem. Phys. Lett.* **2012**, *531*, 126–131.

20. Yan, B.; Thubagere, A.; Premasiri, W.R.; Ziegler, L.; Negro, L.D.; Reinhard, B.M. Engineered SERS substrates with multiscale signal enhancement: Nanoparticle cluster arrays. *ACS Nano* **2009**, *3*, 1190–1202.
21. Zeng, J.; Xia, X.; Rycenga, M.; Henneghan, P.; Li, Q.; Xia, Y. Successive deposition of silver on silver nanoplates: Lateral vs. vertical growth. *Angew. Chem. Int. Edit.* **2011**, *50*, 244–249.
22. Ramanauskaitė, L.; Snitka, V. Surface enhanced Raman spectroscopy of L-alanyl-L-tryptophan dipeptide adsorbed on Si substrate decorated with triangular silver nanoplates. *Chem. Phys. Lett.* **2015**, *623*, 46–50.
23. Leopold, N.; Lendl, B. A new method for fast preparation of highly surface-enhanced Raman scattering (SERS) active silver colloids at room temperature by reduction of silver nitrate with hydroxylamine hydrochloride. *J. Chem. Phys. B* **2003**, *107*, 5723–5727.
24. Liu, J.; White, I.; Devoe, D.L. Nanoparticles-functionalized porous polymer monolith detection elements for surface-enhanced Raman scattering. *Anal. Chem.* **2011**, *83*, 2119–2124.
25. Doak, J.; Gupta, R.K.; Manivannan, K.; Ghosh, K.; Kahol, P.K. Effect of particle size distributions on absorbance spectra of gold nanoparticles. *Phys. E* **2010**, *42*, 1605–1609.
26. Khan, M.A.M.; Kumar, S.; Ahamed, M.; Alrokayan, S.A.; Alsalhi, M.S. Structural and thermal studies of silver nanoparticles and electrical transport study of their thin films. *Nanoscale Res. Lett.* **2011**, *6*, 434–441.
27. Aslan, K.; Lakowicz, J.R.; Geddes, C.D. Rapid deposition of triangular silver nanoplates on planar surfaces: Application to metal-enhanced fluorescence. *J. Chem. Phys. B* **2005**, *109*, 6247–6251.
28. Gooding, J.J.; Ciampi, S. The molecular level modification of surfaces: From self-assembled monolayers to complex molecular assemblies. *Chem. Soc. Rev.* **2011**, *40*, 2704–2718.
29. Zhu, M.; Lerum, M.Z.; Chen, W. How to prepare reproducible, homogeneous, and hydrolytically stable aminosilane-derived layers on silica. *Langmuir* **2012**, *28*, 416–423.
30. Enders, D.; Nagao, T.; Pucci, A.; Nakayama, T. Reversible adsorption of Au nanoparticles on SiO₂/Si: An *in situ* ATR-IR study. *Surf. Sci.* **2006**, *600*, 71–75.
31. Kooij, E.S.; Brouwer, E.A.M.; Wormeester, H.; Poelsema, B. Ionic strength mediated self-organization of gold nanocrystals: An AFM study. *Langmuir* **2002**, *18*, 7677–7682.
32. Zhang, Q.; Li, N.; Goebel, J.; Lu, Z.; Yin, Y. A systematic study of the synthesis of silver nanoplates: Is citrate a “Magic” Reagent? *J. Am. Chem. Soc.* **2011**, *133*, 18931–18939.
33. Xia, X.; Zeng, J.; Zhang, Q.; Moran, C.H.; Xia, Y. Recent developments in shape-controlled synthesis of silver nanocrystals. *J. Chem. Phys. C* **2012**, *116*, 21647–21656.
34. Jin, R.; Cao, Y.C.; Hao, E.; Metraux, G.S.; Schatz, G.C.; Mirkin, C.A. Controlling anisotropic nanoparticle growth through plasmon excitation. *Nature* **2003**, *425*, 487–490.
35. Yi, Z.; Zhang, J.; He, H.; Xu, X.; Luo, B.; Li, X.; Li, K.; Niu, G.; Tan, X.; Luo, J.; *et al.* Convenient synthesis of silver nanoplates with adjustable size through seed mediated growth approach. *Trans. Nonferrous Met. Soc. China* **2012**, *22*, 865–872.
36. Howarter, J.A.; Youngblood, J.P. Optimization of silica silanization by 3-aminopropyltriethoxysilane. *Langmuir* **2006**, *22*, 11142–11147.

37. Klug, J.; Pérez, L.A.; Coronado, E.A.; Lacconi, G.I. Chemical and electrochemical oxidation of silicon surfaces functionalized with APTES: The role of surface roughness in the AuNPs anchoring kinetics. *J. Chem. Phys. C* **2013**, *117*, 11317–11327.
38. Scarpettini, A.F.; Bragas, A.V. Coverage and aggregation of gold nanoparticles on silanized glasses. *Langmuir* **2010**, *26*, 15948–15953.
39. Wei, H.; Eilers, H. From silver nanoparticles to thin films: Evolution of microstructures and electrical conduction on glass substrates. *J. Phys. Chem. Solids* **2009**, *70*, 459–465.
40. Yao, W.; Wang, S.; Wang, H. *Method for Detecting BPA by Surface Enhanced Raman Spectroscopy*; Patent Application Publication: Alexandria, VA, USA, 2012.

© 2015 by the authors; licensee MDPI, Basel, Switzerland. This article is an open access article distributed under the terms and conditions of the Creative Commons Attribution license (<http://creativecommons.org/licenses/by/4.0/>).